Journal of Chromatography A, 1217 (2010) 6484–6495

Contents lists available at ScienceDirect

Journal of Chromatography A

journal homepage: www.elsevier.com/locate/chroma

Unique selectivity windows using selective displacers/eluents and mobile phase modifiers on hydroxyapatite

Christopher J. Morrison[a], Pete Gagnon[b], Steven M. Cramer[a,*]

[a] Department of Chemical and Biological Engineering, Center for Biotechnology and Interdisciplinary Studies, Rensselaer Polytechnic Institute, 110 8th Street, Troy, NY 12180, USA
[b] Validated Biosystems, 240 Avenida Vista Montana, Ste. 7F, San Clemente, CA 92672, USA

ARTICLE INFO

Article history:
Received 26 April 2010
Received in revised form 9 August 2010
Accepted 12 August 2010
Available online 21 August 2010

Keywords:
Hydroxyapatite
Selective displacement
High-throughput screening

ABSTRACT

A detailed study was carried out to combine the unique selectivity of ceramic hydroxyapatite (CHA) with the separation power of selective displacement chromatography. A robotic liquid handling system was employed to carry out a parallel batch screen on a displacer library made up of analogous compounds. By incorporating positively charged, metal chelating and/or hydrogen bonding groups into the design of the displacer, specific interaction sites on CHA were targeted, thus augmenting the selectivity of the separation. The effect of different mobile phase modifiers, such as phosphate, sulfate, lactate and borate, were also investigated. Important functional group moieties and trends for the design of CHA displacers were established. Selective batch separations were achieved between multiple protein pairs which were unable to be resolved using linear gradient techniques, demonstrating the applicability of this technique to multiple protein systems. The specific interaction moieties used on the selective displacer were found to dictate which protein was selectively displaced in the separation, a degree of control not possible using a mono-interaction type resin in displacement chromatography. Mobile phase modifiers were also shown to play a crucial role, augmenting the selectivity of a displacer in a synergistic fashion. Column separations were carried out using selective displacers and mobile phase modifiers identified in the batch experiments, and baseline separation of the previously unresolved protein pairs was achieved. Further, the elution order in these systems was able to be reversed while still maintaining baseline separations. This work establishes a new class of separations which combine the selectivities of multi-modal resins, displacers/eluents, and mobile phase modifiers to create unique selectivity windows unattainable using traditional modes of operation.

1. Introduction

Displacement chromatography is a powerful separation technique that enables the simultaneous concentration and purification of biomolecules from complex mixtures in a single step [1]. Displacement chromatography has been successfully employed for the purification of proteins on multiple different stationary phases [2–13]. A wide variety of classes of displacers, such as polyelectrolytes [9], polysacchardies [14], low-molecular-mass dendrimers [11], amino acids [15], antibiotics [16] and aminoglycoside-polyamines [17] have been identified for protein displacement separations. Further, the application of low-molecular-weight displacers has attracted attention due to several distinct operational advantages [8].

Selective displacement chromatography utilizes the design of the displacer to move a selected solute or solutes back into the displacer zone, separating them from the displacement train. There are two classes of selective displacers, mass action and chemically selective displacers. Chemically selective displacement has been shown to be caused by a selective binding event between the displacer and the protein which is retained in the displacer zone [18–22]. Mass action selective displacers typically have an affinity for the resin that lies between that of the two solutes being separated and can be readily predicted using the steric mass action formalism [23,24]. While selective displacement chromatography has been successfully employed in ion exchange systems [5,9,11,14–17,24–38], to date it has not been applied to CHA or any other multi-modal resin system.

Hydroxyapatite chromatography has recently garnered much attention due to its inherent unique selectivity which is unavailable on any other stationary phase [39]. In particular, ceramic hydroxyapatite (CHA) has been shown to be an effective means to purify large quantities of monoclonal antibodies from associated aggregates, currently unmatched by any other technique [39,40]. Hydroxyapatite exists as a crystalline structure of associated calcium, phosphate and hydroxyl groups, with a chemical formula of $Ca_{10}(PO_4)_6(OH)_2$. Thus, CHA is considered to be a multi-modal type chromatographic resin, due to multiple interaction modes possible

* Corresponding author. Tel.: +1 518 2766198; fax: +1 518 2764030.
E-mail address: crames@rpi.edu (S.M. Cramer).

0021-9673/$ – see front matter © 2010 Elsevier B.V. All rights reserved.
doi:10.1016/j.chroma.2010.08.038

between a protein and the resin surface. Two specific interaction modes have been shown to be dominant for protein adsorption in CHA, namely, cation exchange (between a protein's surface amines and the resin phosphate groups) and metal chelation (between a protein's surface carboxyl groups and the resin calcium sites) [41–45]. Hydrogen bonding with the resin's hydroxyl groups and anion exchange with the resin's calcium sites can also occur; however, these interactions are thought to play a less important role for protein adsorption in CHA [41,45]. The presence of different mobile phase modifiers, such as sodium phosphate, has also been shown to play a critical role in separations on CHA [39,43,44].

While traditional displacement chromatography has been previously attempted on CHA, these separations lacked sufficient resolution between the protein zones [2,46,47]. This paper addresses several questions related to selective displacement in CHA such as: what chemical design motifs make for an effective displacer on CHA, what are the effects of different mobile phase modifiers on the separations, and can selective displacement/elution chromatography be employed to increase the selectivity of CHA? A robotic high-throughput screen previously developed in our laboratory [22] was employed to examine the utility of a displacer library spanning the different interaction modes involved in CHA adsorption and the effect of different mobile phase modifiers on these separations were examined. Important functional group moieties and trends for the design of CHA displacers were established and selective batch separations were achieved between multiple protein pairs which were unable to be resolved using linear gradient techniques. Finally, column separations were carried out based upon the batch results, demonstrating the power of this technique when operated in the column mode.

2. Experimental

2.1. Materials

Ceramic hydroxyapatite (CHA), type I, 40 μm was donated and purchased from Bio-Rad (Hercules, CA). Pharmacia empty glass columns (4.6 mm × 100 mm, 4.6 mm × 50 mm) and a 50 mL Superloop were purchased from GE Healthcare (Uppsala, Sweden). Ninety-six-well Multiscreen-HV Durapore membrane bottomed plates were purchased from Millipore (Bedford, MA). A Jupiter 5 μm C4 300A column (4.6 mm × 50 mm) was purchased from Phenomenex (Torrance, CA). Ribonuclease A from bovine pancreas (RNaseA), ribonuclease B from bovine pancreas (RNaseB), α-chymotrypsinogen A from bovine pancreas (α-ChyA), cytochrome C from equine heart (CytC), lysozyme from chicken egg white (Lys), conalbumin from chicken egg white (Conal), hemoglobin from bovine blood (Hemo), myoglobin from equine heart (Myo), avidin from chicken egg white, subtilisin A from *Bacillus*, elastase from porcine pancreas, papain from papaya latex, bromelain from pineapple stem, alcohol dehydrogenase from equine liver, trypsinogen from bovine pancreas, catalase from bovine liver, aprotinin from bovine lung, aconitase from porcine heart, albumin from bovine serum, neomycin sulfate (displacer 1), paromomycin sulfate (2), bekanamycin sulfate (3), amikacin sulfate (4), spermine (5), bis(hexamethylene)triamine (7), spermidine (8), 1,4-bis(3-aminopropyl)piperazine (9), diethylenetriamine (10), 4,7,10-trioxa-1,13-tridecanediamine (11), N,N′-diethyl-1,3-propanediamine (12), N,N-diethyldiethylenetriamine (13), 2-(2-aminoethylamino)ethanol (14), spectinomycin dihydrochloride pentahydrate (15), L-arginine methyl ester dihydrochloride (16), L-lysine methyl ester dihydrochloride (17), N-hexylethylenediamine (18), piperazine (19), cyclohexylamine (20), acetic acid (21), malonic acid (22), succinic acid (23), adipic acid (24), isocitric acid lactone (25), *trans*-aconitic acid (26), 1,2,4-butanetricarboxylic acid (27), 1,2,3,4-butanetetracarboxylic acid (28), glycine (29), 3-guanidinopropionic acid (30), 5-aminovaleric acid (31), pantothenic acid (32), aspartic acid (33), L-β-homoglutamic acid hydrochloride (34), guanidinosuccinic acid (35), L-2,3-diaminopropionic acid hydrochloride (36), lysine (37), arginine (38), *meso*-2,3,-diaminosuccinic acid (39), ethylenediaminetetrapropionic acid (40), glycerol (41), threitol (42), adonitol (43), dulcitol (44), malic acid (45), tartaric acid (46), mucic acid (47), arabic acid (48), 1-(2-hydroxyethyl)piperazine (49), 1,4-bis(2-hydroxyethyl)piperazine (50), N,N′-bis(2-hydroxyethyl)ethylenediamine (51), 3-amino-1,2-propanediol (52), ethylenediamine (53), piperazine-2-carboxylic acid dihydrochloride (54), ethylenediamine-N,N′-diacetic acid (55), sodium phosphate (monobasic and dibasic), sodium sulfate, boric acid, lactic acid, potassium phosphate (dibasic), sodium chloride, bis–tris, hydrochloric acid, sodium hydroxide, acetonitrile (ACN), trifluoroacetic acid (TFA), acetone and fluorescamine were purchased from Sigma–Aldrich (St. Louis, MO). PE-NH_2 (displacer 6) was synthesized in Prof. Moore's laboratory at Rensselaer Polytechnic Institute (Troy, NY) as described elsewhere [36]. All other unlisted chemicals were obtained from Sigma–Aldrich. All reagents and solvents were used as received without further purification.

2.2. Equipment

High-throughput batch screening experiments were carried out on a Biomek 2000 robotic liquid handling system from Beckman Coulter (Fullerton, CA). Supernatant solutions were collected from the membrane plates using a vacuum manifold donated by Millipore. Supernatant solutions from the membrane plates were analyzed using a HTS 7000 Bio Assay Plate Reader from PerkinElmer (Waltham, MA). Column separations and fraction analysis were carried out on an HPLC system consisting of a 600E HPLC pump and controller, a 717 plus autoinjector and a 484 absorbance detector from Waters (Milford, MA). The HPLC system utilized Millennium v.2.15.01 software and data acquisition, also from Waters. Fractions from the column runs were collected using an Advantec SF-2120 autosampler (Tokyo, Japan).

2.3. Procedures

2.3.1. Linear gradient experiments

An empty column (4.6 mm × 50 mm) was first packed with CHA resin. All proteins were then screened on this column using different linear gradients and running buffers. A linear gradient of phosphate was carried out on the protein library with an A buffer of 5 mM sodium phosphate at pH 6.5, a B buffer of 500 mM sodium phosphate at pH 6.5, and a C regeneration buffer of 0.5 M potassium phosphate with 1 M sodium chloride at pH 10. The column was first pre-equilibrated with 100% A, followed by a linear gradient of 0–100% B in 30 column volumes, followed by 100% C for 4 column volumes.

Sodium chloride linear gradients were also carried out on the protein library in the presence of different sodium phosphate concentrations. These experiments were run using an A buffer of 5, 10 or 20 mM sodium phosphate at pH 6.5, a B buffer of 1 M sodium chloride with the appropriate concentration of sodium phosphate used in A at pH 6.5, and a C regeneration buffer of 0.5 M potassium phosphate with 1 M sodium chloride at pH 10. The column was first pre-equilibrated with 100% A, followed by a linear gradient of 0–100% B in 30 column volumes, followed by 100% C for 4 column volumes.

Alternative mobile phase modifier gradients were also carried out on the Lys/RNaseA protein pair using monobasic sodium phosphate, sodium sulfate, lactate or borate as the modifier. These experiments were run using an A buffer of 5 mM bis–tris, 10 mM

MOPS and 10 mM MES at pH 6.5, a B buffer of 500 mM mobile phase modifier in buffer A at pH 6.5, and a C regeneration buffer of 0.5 M potassium phosphate with 1 M sodium chloride at pH 10. The column was first pre-equilibrated with 100% A, followed by a linear gradient of 0–100% B in 35 column volumes, followed by 100% C for 5 column volumes. For all linear gradient experiments the flow rate was 1 mL/min, the column effluent was monitored at 280 nm and 40 μL of 1–2 mg/mL protein solution was injected.

2.3.2. High-throughput batch screen of the displacer library

A robotic HTS protocol that had been previously developed was used to determine the performance of the displacer library on CHA [22]. The bulk stationary phase (CHA) was first washed twice with deionized water and then twice with the appropriate buffer. Buffers for the batch displacement runs were either 5, 10 or 20 mM sodium phosphate, pH 6.5. Once washed, the supernatant liquid was removed and 6 mL of wet, settled stationary phase slurry was equilibrated with 72 mL of a single protein mixture at a concentration of 5 mg/mL (in the appropriate buffer). The protein solution was equilibrated with the resin for 10 h, during which the stationary phase was allowed to settle under gravity. Upon settling, the supernatant liquid was removed and the protein content in the supernatant solution was determined by reversed-phase liquid chromatography (RPLC) analysis (see below). The mass of protein adsorbed on the stationary phase was then calculated by mass balance.

The protein-saturated resin was then re-suspended as a 50:50 (v/v) slurry using some of the previously removed supernatant from the protein loading step (to prevent any desorption). This resin slurry was then loaded onto 96-well membrane plates using a repeating pipette, dispensing 20 μL of slurry per well. (*Note*: due to the relatively fast settling velocity of the CHA resin the Biomek machine was unable to reliably dispense a 50:50 slurry mixture; thus a manual dispense method was used.) A vacuum manifold was used to filter the slurries through the membrane plate, leaving 10 μL of settled wet resin in each well. These plates were then loaded onto the Biomek machine. In addition, 30 mM solutions of each displacer (in the appropriate buffer) were loaded into separate reservoirs on the Biomek, and the appropriate buffer was loaded into its own reservoir. A premade protocol was then employed to run the batch screen. The Biomek performed serial dilutions of each displacer and then dispensed 120 μL of 30, 20, 10 or 5 mM displacer solutions into each individual well. Each displacer concentration, with the appropriate phosphate buffer concentration, was done in triplicate. After all solutions were loaded into the wells, the suspensions were mixed by repeated pipetting and allowed to equilibrate for 5 h. After equilibration the supernatant solutions from the wells were collected for analysis using the vacuum manifold.

2.3.3. Analysis of the batch supernatant solutions

After collection, the supernatants were analyzed using a plate reader or RPLC. Supernatants that contained displacers which did not adsorb at 280 nm were diluted twofold to increase sample volume, placed into a quartz 96-well plate and analyzed at 280 nm absorbance using a plate reader. Calibration curves were created by measuring the absorbance of known protein concentrations in the appropriate buffer. For those few supernatants that contained displacers with adsorption at 280 nm (only 2 displacers of 55), it was necessary to separate the displacer and protein before analysis. RPLC was carried out using a C4 column (4.6 mm × 50 mm) with an A buffer of deionized water with 0.1% TFA and a B buffer of 90% ACN, 10% deionized water and 0.1% TFA (all v/v). The column was first pre-equilibrated with 100% A. A linear gradient was then carried out from 0 to 100% B in 5 column volumes followed by 100% B for 1 column volume. The flow rate was 1 mL/min, the column effluent was monitored by 280 nm and 40 μL of the supernatants were injected. This RPLC protocol was also used to analyze the supernatants from the resin protein loading step.

2.3.4. High-throughput batch experiments using different mobile phase modifiers

For these batch experiments different mobile phase modifiers were used in addition to a common background buffer to maintain pH. The modifiers sodium phosphate (monobasic), sodium sulfate, lactic acid (lactate) and boric acid (borate) were used at concentrations of 5, 10 and 20 mM. The salt bis–tris was used as a common background buffer for all modifiers at a concentration of 5 mM to maintain a pH of 6.5. Proteins were loaded onto the CHA resin in a suspension of the appropriate modifier and background pH buffer. Displacer solutions were also made in the appropriate suspension as well. The HTS protocol outlined in procedure 2 was used for the batch experiments (with these modifications) for the different mobile phase modifiers. Analysis of the resulting supernatants was carried out using the plate reader protocol outlined in procedure 3.

2.3.5. Column displacements on ceramic hydroxyapatite

For the displacement experiments a CHA column (4.6 mm × 121.5 mm or 4.6 mm × 60 mm) was initially equilibrated with the appropriate carrier buffer being used. The column was then perfused sequentially with feed, displacer and regeneratant solutions. A 50 mL superloop was used to feed the column with the displacer solution in order to provide a continuous flow of displacer at a constant concentration. The experimental conditions, such as feed load, flow rate, displacer concentration and carrier buffer can be found in the figure captions. Regeneration was carried out using a linear gradient from the carrier buffer to the regeneration buffer (500 mM potassium phosphate, 850 mM sodium chloride, pH 10.5). (*Note*: the efficacy of this regeneration protocol was found to be effective at removing all of the bound displacers which bound to CHA using only electrostatic or hydrogen bonding interactions [such as displacers 8 and 16]). Fractions of the column effluent (300 μL) were collected during the displacement experiment for subsequent analysis.

2.3.6. Analysis of the column effluent fractions

Fractions were analyzed using RPLC which was carried out using the same column and buffers described in procedure 3. The column was first pre-equilibrated with 100% A. A linear gradient was then carried out from 0 to 100% B in 30 column volumes followed by 100% B for 2.5 column volumes. The flow rate was 1 mL/min, the column effluent was monitored by UV (either 214 or 280 nm) and 40 μL portions of the fractions were injected. This protocol resulted in the detection of both proteins and displacer (aside for displacer 8). For displacer 8 a duplicate displacement experiment was carried out in the same manner as before without loading protein. Fractions from this experiment were then labeled using fluorescamine. A solution of 0.28 mg/mL of fluorescamine in acetone was added to the fractions in a 3:1 ratio (sample:fluorescamine solution). Analysis of the fractions was then carried out using the plate reader monitoring adsorbance at 280 nm. Due to the reproducible nature of the column displacement, this secondary experiment (with no load) was then used to determine the displacer breakthough profile in the column separation which used protein.

3. Results and discussion

3.1. Identification of model protein systems for ceramic hydroxyapatite

In order to evaluate low-molecular-weight compounds as potential selective displacers and to evaluate their efficacy for CHA,

Table 1
Retention times (in min) for various proteins on CHA using a sodium chloride gradient (with buffer concentrations of 5, 10 and 20 mM sodium phosphate) or a sodium phosphate gradient (with a starting buffer concentration of 5 mM sodium phosphate). Protein abbreviations and isoelectric points are also given. Inseparable proteins using a sodium chloride gradient are denoted by blue, inseparable proteins using a phosphate gradient are denoted by red, and protein pairs inseparable by both gradient methods are shown in separate violet box.

Protein	Isoelectric point	NaCl Grad 5 mM Phos	NaCl Grad 10 mM Phos	NaCl Grad 20 mM Phos	Protein	Phos Grad 5 mM Phos
α-chymotrypsinogen A (α-ChyA)	9.0	15.3	15.3	15.1	RNaseB	14.1
ribonuclease B (RNaseB)	9.7	14.7	14.2	13.8	Myo	16.1
lysozyme (Lys)	11.6	13.8	13.5	13.7	Conal	16.8
ribonuclease A (RNaseA)	9.6	16.2	15.4	15.6	RNaseA	17.0
myoglobin (Myo)	7.2	26.9	22.1	15.4	Lys	17.6
hemoglobin (Hemo)	6.8	22.8	22.4	18.8	Hemo	19.2
cytochrome C (CytC)	10.3	24.4	23.6	22.8	α-ChyA	19.6
conalbumin (Conal)	6.1	40.8	32.6	21.5	CytC	27.8

appropriate model protein systems were required. Thus, a protein library was screened for retention behavior in different linear gradient experiments on CHA. Both phosphate and sodium chloride gradient experiments were carried out at pH 6.5. The sodium chloride gradient experiments were also repeated in the presence of different sodium phosphate concentrations (namely 5, 10 and 20 mM) in order to determine a protein's sensitivity to phosphate. From these data a number of proteins were chosen which represented a range of different retention times in both of the linear gradient experiments as well as different sensitivities to phosphate concentration in the sodium chloride gradient (Table 1). The resulting proteins thus provide an array of different interaction strengths for both primary modes of protein interaction with the CHA resin (i.e. cation exchange and metal chelation). In this work these proteins were then employed to evaluate displacer efficacy in CHA.

In order to investigate the separation power of selective displacement on CHA, it was also necessary to identify proteins pairs that were inseparable by linear gradient chromatography. Table 1 also shows a number of protein pairs which were inseparable by either a sodium chloride gradient (blue) or phosphate gradient (red). Further, two pairs were identified which were inseparable by both gradient techniques (violet). RNaseA/Myo was unresolved using a phosphate gradient or with a sodium chloride gradient containing 20 mM sodium phosphate. RNaseA/Lys was unresolved for all sodium chloride and phosphate gradients. It should be noted that even though the retentions of these proteins were separated by more than 1 min in some cases (Table 1), the peaks of these proteins completely overlapped (see Fig. 1). Thus, these two protein pairs represented very challenging separations on the CHA stationary phase material and were employed in our high-throughput evaluation of displacer selectivity.

3.2. Design and efficacy evaluation of a low-molecular-weight displacer library for CHA

In order to obtain a deeper understanding of the displacer chemistry required for high efficacy and/or selectivity on CHA, a displacer library of 55 commercially available molecules was evaluated using a robotic high-throughput batch screen on the proteins listed in Table 1. Example structures of the displacer molecules are shown in Fig. 2 (*Note*: while the molecules used in the batch screen may be considered to be either displacers or eluents based upon their performance in the column mode, for the sake of simplicity they will be referred to primarily as "displacers").

The dominant modes of interaction for protein binding on CHA are cation exchange with phosphate sites (P site interactions) and metal chelation with the calcium sites (C site interactions). Two

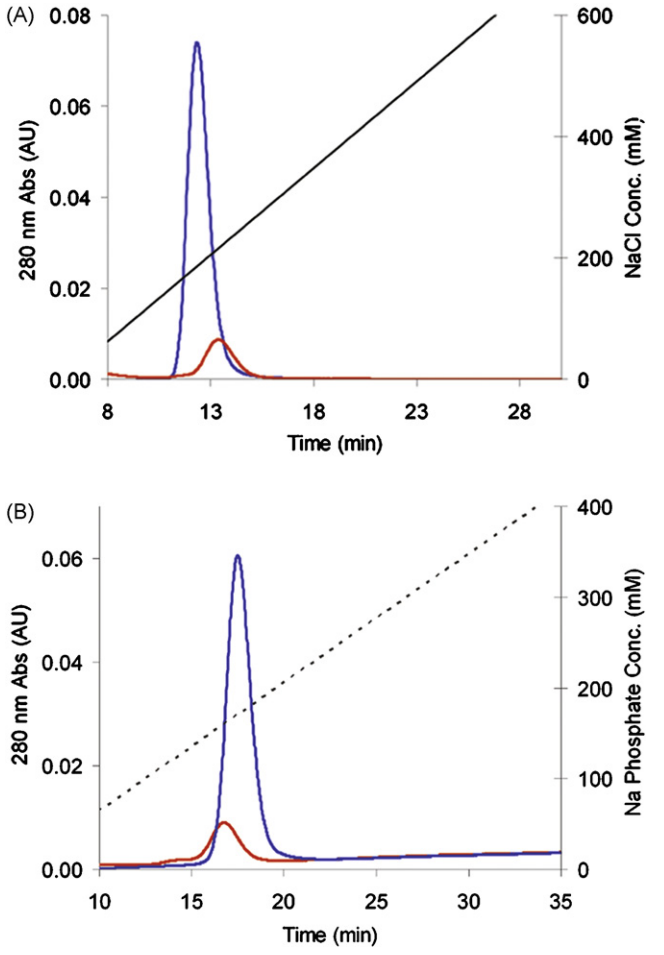

Fig. 1. Chromatograms of RNaseA (red) and Lys (blue) on CHA using different linear gradients. (A) Sodium chloride gradient (solid black) with a 5 mM sodium phosphate buffer. (B) Sodium phosphate gradient (dashed black) also with a 5 mM sodium phosphate buffer. (For interpretation of the references to colour in this figure legend, the reader is referred to the web version of the article.)

other minor interaction modes are also possible, namely hydrogen bonding and anion exchange. As can be seen in Fig. 2 these different types of interactions were taken into account in the overall design of the displacer library. The 55 molecule library was split into multiple categories of design based upon the different resin interactions possible with the displacer. For example, the category shown in Fig. 2A is made up of molecules which should interact with the resin primarily via cation exchange, while the category shown in Fig. 2B consists of molecules which could interact by cation exchange and/or metal chelation. The library was also designed to include molecular analogues both within and between different categories of design (denoted by red or blue arrows, respectively, in Fig. 2). For example, displacer 37 is an analogue of displacer 17, where the former is capable of both cation exchange and metal chelation, while the latter (with a methylated carboxyl group) is only capable of cation exchange interactions. By constructing the displacer library with different categories of design and molecular analogues, differences in displacement/elution behavior are able to be directly related to differences in the chemical structure.

The proteins in Table 1 were evaluated in an extensive high-throughput batch screen using the displacer library depicted in Fig. 2 as described in Section 2. Further, since previous studies have demonstrated the importance of mobile phase composition on CHA chromatography, specifically phosphate concentrations [39,40,48], the robotic screening experiments were carried out at

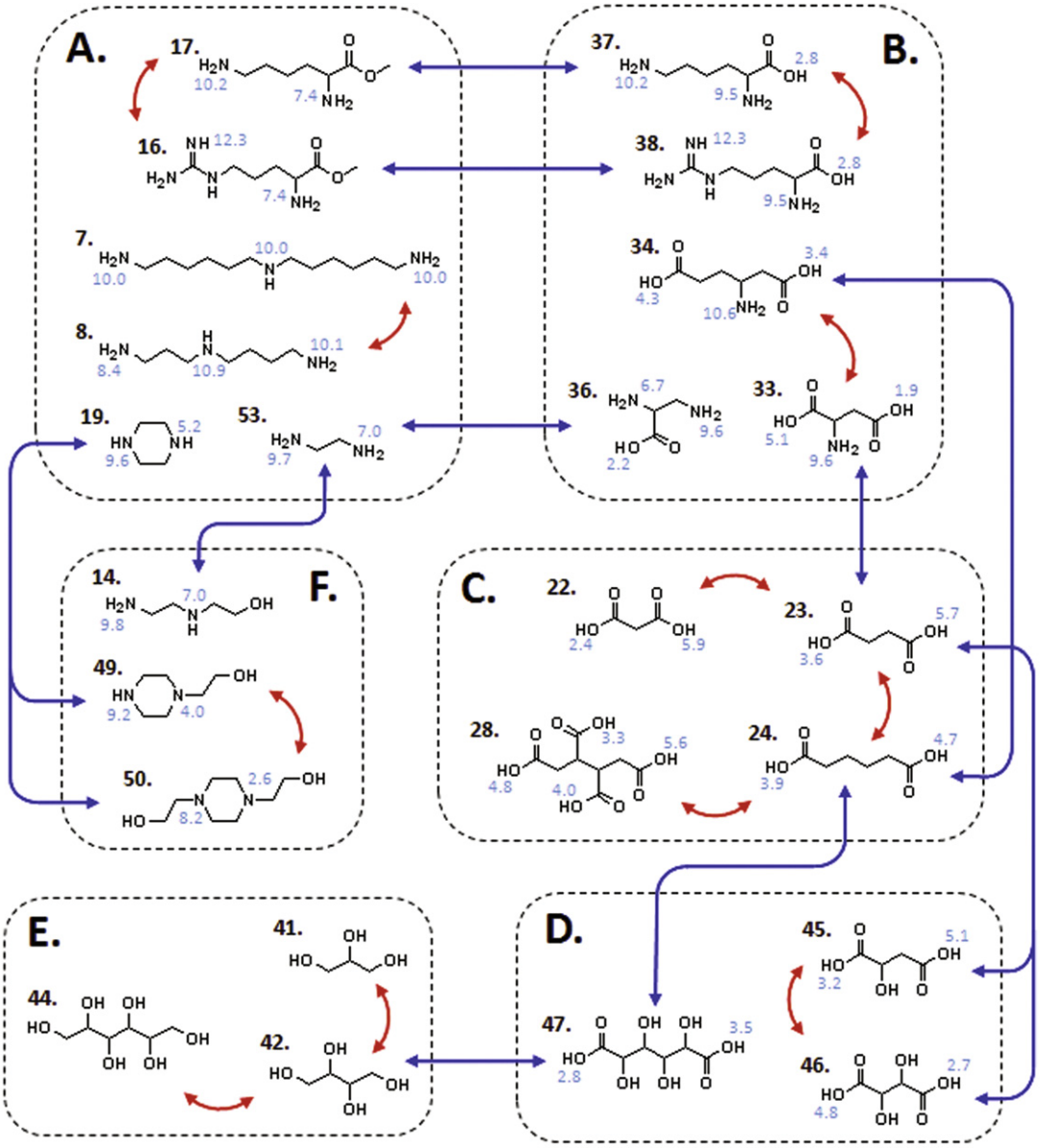

Fig. 2. Example structures from the displacer library screened on CHA. Displacers are grouped into different categories based upon the resin interaction moieties used in their design: (A) primarily cation exchange; (B) mix of cation exchange and metal chelation; (C) primarily metal chelation; (D) mix of metal chelation and hydrogen bonding; (E) primarily hydrogen bonding; (F) mix of cation exchange and hydrogen bonding. Displacer analogues within a single category of design are shown by red arrows, while displacer analogues between different categories of design are shown by blue arrows. Individual ammonium salt and carboxyl group pK_a values (determined using the ChemAxon Marvin Calculator [53]) are shown in light blue. Displacer structures are labeled as described in Section 2.1. (For interpretation of the references to colour in this figure legend, the reader is referred to the web version of the article.)

various sodium phosphate buffer concentrations (5, 10 and 20 mM) at pH 6.5. This large set of data was then examined to provide insight into both displacer design and protein selectivity in CHA displacement/elution systems.

3.2.1. *Effect of distance between interaction moieties on displacers*

Previous work in our laboratory has shown that the separation distance between resin interaction moieties on a displacer can have a significant impact on the overall displacer performance in ion exchange (e.g. by varying charge density) [21]. However, this work was done on a mono-interaction type resin with a ligand which had some mobility with respect to the resin surface. For CHA resins, multiple types of interaction sites are possible, and these sites are presented in a fixed crystalline lattice structure with specific distances between different interaction sites. It should also be noted that metal chelation is considered to be more of a "close range" interaction, whereas electrostatic interactions can take place over much longer distances. It is hypothesized that the spacing of interaction moieties on a displacer would have a significant effect on a displacer's efficacy for CHA. In order to investigate these effects, several analogues which only differed in their respective spacing between similar interaction moieties were compared.

Data from these batch protein displacement experiments are presented as displacer efficacy comparison plots (e.g. Fig. 3). These plots present a histogram of the difference in percent protein displaced between two displacer analogues for a variety of conditions (e.g. different proteins, phosphate concentrations). The individual bars are grouped together, with each grouping representing a specific protein and phosphate concentration which was used in the robotic batch screen (*Note*: all data was obtained from triplicate

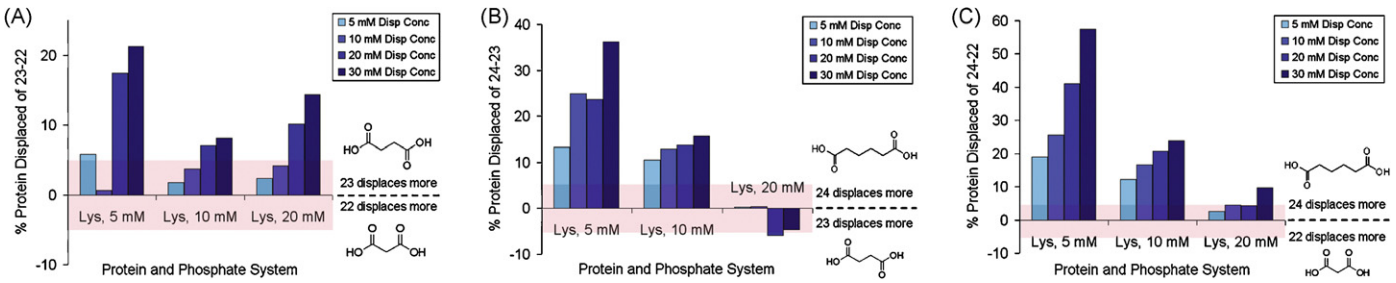

Fig. 3. Displacer efficacy comparison plots for the analysis of different separation distances between two carboxyl groups for displacing Lys at different phosphate concentrations (5, 10 and 20 mM). The pink bar denotes a ±5% error in displacement values. (A) Comparison between a one carbon (displacer 22) and two carbon (displacer 23) separation distance; (B) comparison between a two carbon (displacer 23) and four carbon (displacer 24) separation distance; (C) comparison between a one carbon (displacer 22) and four carbon (displacer 24) separation distance. (For interpretation of the references to colour in this figure legend, the reader is referred to the web version of the article.)

experiments). The individual bars within each grouping represent a specific concentration of displacer which was used for that data point (see figure legends for details). Finally, the specific structures of the analogues being compared are shown either above or below the *x*-axis. If a given bar value is positive, then the analogue shown above the *x*-axis displaced more protein (at the given mobile phase condition) than the analogue depicted below the *x*-axis. This would then imply a higher efficacy for displacing this particular protein from the CHA resin. A very large set of data was obtained using this screen and representative data will now be presented to illustrate important trends.

In order to first analyze the effect of separation distance between different carboxyl groups on a displacer, a two carboxyl group moiety is presented as an example case. Three analogues with a 1, 2 or 4 carbon spacing between the carboxyl groups (displacers 22, 23 and 24, respectively) are compared for their ability to displace Lys at various phosphate concentrations (Fig. 3). Fig. 3A compares a one carbon spacing vs. a two carbon spacing. As can be seen in the figure, the larger separation distance was able to displace more Lys for all three phosphate concentrations. This trend continues for most of the comparisons between a two and four carbon spacing (Fig. 3B), and a one and four carbon spacing (Fig. 3C). Clearly, as the distance between the two carboxyl groups increases, more Lys is effectively displaced. This suggests that the displacer efficacy for CHA increases with increasing distance between carboxyl groups on the displacer. This is especially apparent for the Lys, 5 mM phosphate condition in parts A (one carbon difference), B (two carbon difference) and C (three carbon difference) of Fig. 3. It should be noted that this trend was also seen for the other proteins employed in the robotic batch screen. Another trend shown in Fig. 3 (and other carboxyl based analogue comparisons) is that as the phosphate concentration increased, the relative difference in percent protein displaced between the two analogues decreased. This is explained by the fact that phosphate directly mitigates metal chelation interactions. Thus, as the phosphate concentration increases, the strength of the metal chelation interaction decreases. The analogues examined in Fig. 3 are then unable to effectively displace proteins regardless of the spacing between the carboxyl groups, thereby decreasing the difference in efficacy between the two analogues shown in the efficacy comparison plots.

We hypothesize that the increased efficacy seen due to an increased separation distance between carboxyl groups relates to the geometric alignment of these moieties with the fixed calcium sites on the CHA surface. Upon analysis of the CHA crystal lattice [48–50] it can be seen that the distances between different calcium sites on the CHA surface occur at approximately 4, 6 and 9 Å (*Note*: distances greater than 9 Å occur but are not relevant here). Using computer software [51] (with MM2 energy minimization) the rough distances between the alpha carbons of the two carboxyl groups on the displacers were determined to be as follows: displacer 22–2.5 Å, displacer 23–4 Å and displacer 24–6.5 Å. If the shortest distance between two adjacent calcium sites on the CHA surface is only 4 Å then the two carboxyl groups of displacer 22 would be unable to interact with two unique calcium sites. Thus, only one of the carboxyl groups of displacer 22 should be able to interact with the CHA surface at a given time. On the other hand, displacer 23 (with a 4 Å separation distance) could possibly interact with two unique calcium sites on the CHA surface. This would enable multi-point binding (or avidity) which would effectively increase displacer 23's efficacy for CHA relative to displacer 22. Finally, displacer 24 (with a 6.5 Å separation distance) would be able to interact not only with two calcium sites that are separated by 4 Å, but also with those separated by 6 Å, thereby increasing the total number of possible avidity binding sites available to displacer 24. This could effectively increase displacer 24's efficacy over displacer 23. This hypothesis would explain the behavior seen in the carboxyl based displacer comparisons, where an increased separation distance between carboxyl groups affords a higher efficacy due to increased avidity and number of possible binding sites.

Fig. 4 examines effect of separation distance between positively charged groups on a displacer, specifically displacers 7 and 8 on the ability to displace three proteins (Lys, α-ChyA and CytC). As can be seen in the figure, the displacer with the shorter separation distance (displacer 8) was much more effective at displacing all three proteins at various phosphate concentrations. This trend was also seen for all of the other proteins examined in the robotic batch screen (results not shown). As the distance between charge groups decrease on the displacer, the overall charge density on the displacer increases, resulting in a higher displacer efficacy due to increased strength of electrostatic interactions with the CHA surface. Previous work in our laboratory on IEX displacer design yielded similar results, where an increase in charge density resulted in increased displacer efficacy [19,21,22]. Thus, unlike metal chelation interactions where an increase in separation distance resulted in increased CHA efficacy, a decrease in separation distance between positively charge groups resulted in increased CHA efficacy due to a higher charge density. It should also be noted that the phosphate concentration did not significantly affect the overall difference in percent protein displaced values shown in Fig. 4. This makes sense since the minor change in phosphate concentration (15 mM) would not be expected to have a significant effect on electrostatic interactions. This is in contrast to the results seen in Fig. 3 with the metal chelation dominant displacers.

3.2.2. Single-interaction moiety vs. multi-interaction moiety displacers

Previous studies have shown that proteins can interact with CHA through cation exchange, metal chelation or a mixture of both interaction modes [42–44,52]. Thus, the displacement behavior of a molecule which affects only one interaction mode could be

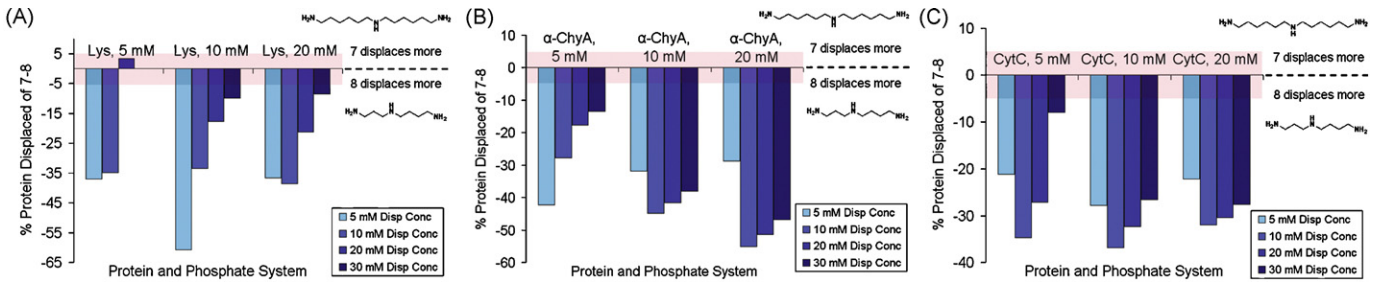

Fig. 4. Displacer efficacy comparison plots for the analysis of different separation distances between three amine groups using different proteins, and phosphate concentrations (5, 10 and 20 mM). Displacers 7 and 8 are used. The pink bar denotes a ±5% error in displacement values. (A) Comparison using Lys; (B) comparison using α-ChyA; (C) comparison using CytC. (For interpretation of the references to colour in this figure legend, the reader is referred to the web version of the article.)

significantly different from one that affects both modes of interaction. In order to investigate these effects, comparisons between single-interaction moiety displacers (Fig. 2A, C, and E) and multi-interaction moiety displacers (Fig. 2B, D, and F) were evaluated. As an example, the addition of positively charged amine groups to displacers containing carboxyl groups was analyzed. Fig. 5 compares the efficacy of displacer 23 (two carboxyls) to displacer 33 (two carboxyls, one primary amine) for displacing the proteins Lys, α-ChyA and CytC.

As can be seen in the figure, displacer 23 (single interaction) was much more effective at displacing all three proteins than displacer 33 (multiple interactions). Interestingly, this result was also seen for the other proteins evaluated in the robotic screen as well as for other analogue comparisons (e.g. displacers 24 and 34). When the library was intially designed it had been hypothesized that by adding another mode of interaction the displacer would be able to partake in a multi-interaction avidity binding to the CHA surface. However, as demonstrated by these analogue comparisons, this was not the case. By adding a charge moiety to the "carboxyl group based" displacer the displacer's efficacy for CHA was actually decreased. A possible explanation for this may be that the different interaction modes of CHA are not mutually exclusive. In other words, a postively charged solute which is attracted to a negatively charged phosphate site on the CHA surface may also be repelled by an adjacent positively charged calcium site. Similiarly, a negatively charged carboxyl group which participates in metal chelation interactions with a postively charged calcium site may also be repelled by an adjacent negatively charged phosphate site. Thus, by adding the amine to the carboxyl based displacer, charge repulsion effects were inadvertantly added to the design, thereby weakening each interaction mode available to the displacer. This resulted in the decreased efficacy seen in Fig. 5. It should be noted that this trend was also seen when comparing amine based displacers to multi-interaction analogues. For example, in comparisons between displacers 17 and 37, and displacers 16 and 38 (see Supplementary Fig. A), the metal chelation potential of the carboxyl group is effectively neutralized through methylation, thereby also removing the negative charge of the carboxyl group. Results from these comparison agreed with the previous trend, where the single-interaction displacer was seen to be much more effective than the multi-interaction displacer for the proteins used in the screen. These results indicate that charge repulsion effects can play a major role in CHA binding for low-molecular-weight displacers.

Although the primary modes of interaction with CHA (cation exchange and metal chelation) can affect each other due to charge repulsion effects, hydrogen bonding with the CHA surface should not affect these modes of interaction. Typically considered to be a minor interaction mode for CHA, the role of hydrogen bonding in CHA is still not well understood. In order to investigate possible hydrogen bonding effects on displacer efficacy, several analogue comparisons were carried out by adding hydroxyl groups to carboxyl or amine based displacers. As an example, Fig. 6 compares displacer 23 (two carboxyls) and displacer 45 (two carboxyls, one hydroxyl) using the proteins Lys, Myo and RNaseA.

As can be seen in Fig. 6A, the protein Lys was more effectively displaced by the single-interaction displacer (23) vs. the multi-interaction displacer (45). This was also seen for the proteins CytC and α-ChyA (results not shown). Clearly, the addition of the hydroxyl group hindered the ability of the two carboxyl moiety displacer to effectively displace these three proteins. On the other hand, as shown in Fig. 6B and C, the multi-interaction displacer (45) was more effective at displacing the protein RNaseA at a 10 mM phosphate and the protein Myo for all phosphate concentrations examined. For these proteins, the addition of the hydroxyl group apparently increased the displacer's ability to effectively displace the protein. This trend, where a carboxyl only displacer was more effective for Lys, CytC and α-ChyA and the carboxyl/hydroxyl combination displacer was more effective for Myo and RNaseA was also observed for several other similar analogue comparisons (e.g. displacer 23 vs. 46, and displacer 24 vs. 47). This behavior is most likely due to differences in the role of hydrogen bonding for each individual protein. Since the carboxyl/hydroxyl combination displacers are able to affect two modes of binding, it is likely that hydrogen

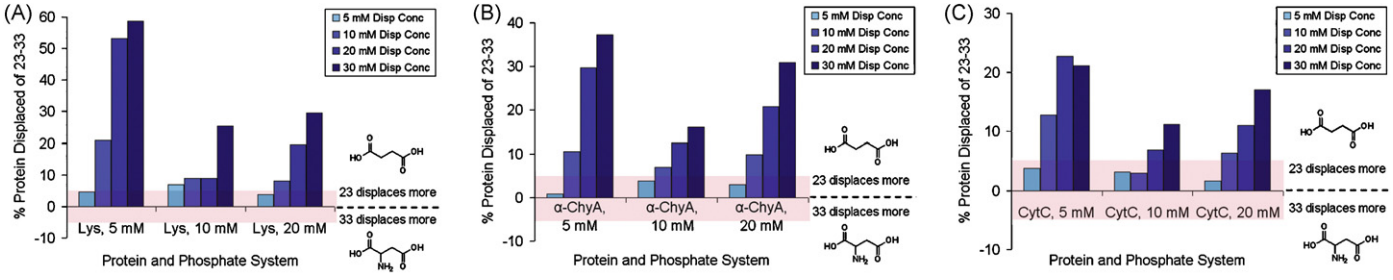

Fig. 5. Displacer efficacy comparison plots for the analysis of charge addition to a two carboxyl group moiety using different proteins and phosphate concentrations (5, 10 and 20 mM). Displacers 23 and 33 are examined. The pink bar denotes a ±5% error in displacement values. (A) Comparison using Lys; (B) comparison using α-ChyA; (C) comparison using CytC. (For interpretation of the references to colour in this figure legend, the reader is referred to the web version of the article.)

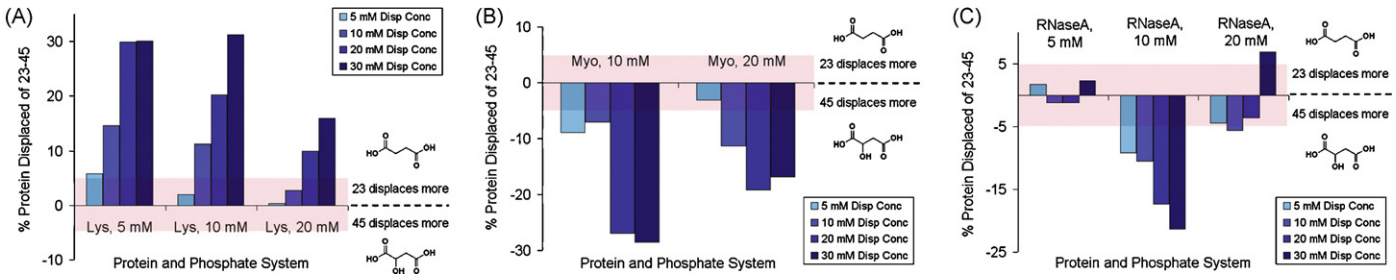

Fig. 6. Displacer efficacy comparison plots for the analysis of hydroxyl addition to a two carboxyl group moiety using different proteins and phosphate concentrations (5, 10 and 20 mM). Displacers 23 and 45 are used. The pink bar denotes a ±5% error in displacement values. (A) Comparison on Lys; (B) comparison on Myo; (C) comparison on RNaseA. (For interpretation of the references to colour in this figure legend, the reader is referred to the web version of the article.)

bonding is playing a role in the interactions of Myo and RNaseA with the CHA surface. A possible explanation for why the addition of a hydroxyl group hindered the displacer's ability to displace Lys, CytC and α-ChyA may be that the hydroxyl group on the displacer interfered with metal chelation (either due to steric effects or through direct interference with the metal chelation bond). The addition of hydroxyl groups to amine based displacers was also evaluated. Several analogue comparisons, such as displacer 53 vs. 14 (see Supplementary Fig. B), displacer 19 vs. 49 and displacer 19 vs. 50, were made. In contrast to the results with the carboxyl based displacers, it was found that the addition of a hydroxyl group to an amine based displacer hindered the ability of the molecule to effectively displace a protein, regardless of which protein or phosphate condition was used. Future work will attempt to shed more light on this behavior.

3.3. Selectivity in batch displacement experiments

The extensive data sets obtained from the robotic high-throughput batch experiments were also examined to identify displacers which gave selective separations in the batch mode for different protein pairs (shown in Table 1). To demonstrate the separation power of selective displacement/elution on CHA it was desired to find displacers which gave a selective separation between Lys and RNaseA, a protein pair which was unable to be resolved by either sodium chloride or phosphate gradients (Fig. 1). The data from these experiments were employed to generate selectivity pathway plots [22] and 3D selectivity plots as shown in Fig. 7. In selectivity pathway plots (Fig. 7A–C), the percentage of one protein displaced from a pair is plotted as a function of the percentage displacement of the other protein. The trajectory is then constructed at increasing displacer concentrations (5–30 mM) and different regions of the plot are defined as being either "selective" (greater than 30% separation between the pair, denoted by the light green triangular region) or "exclusive" (greater than 50% separation between the pair and one protein remains strongly bound onto the resin with less than 10% displaced, denoted by the dark green rectangular region). The different colored trajectories correspond to the different phosphate concentrations used in the experiments. In 3D selectivity plots (Fig. 7D–F), the phosphate concentration used in the experiment is plotted against the displacer concentration. The color contour map laid over this plot corresponds to the percent separation in the protein pair (shown by the color bar), with less than 30% being non-selective (dark blue) and greater than 30% rep-

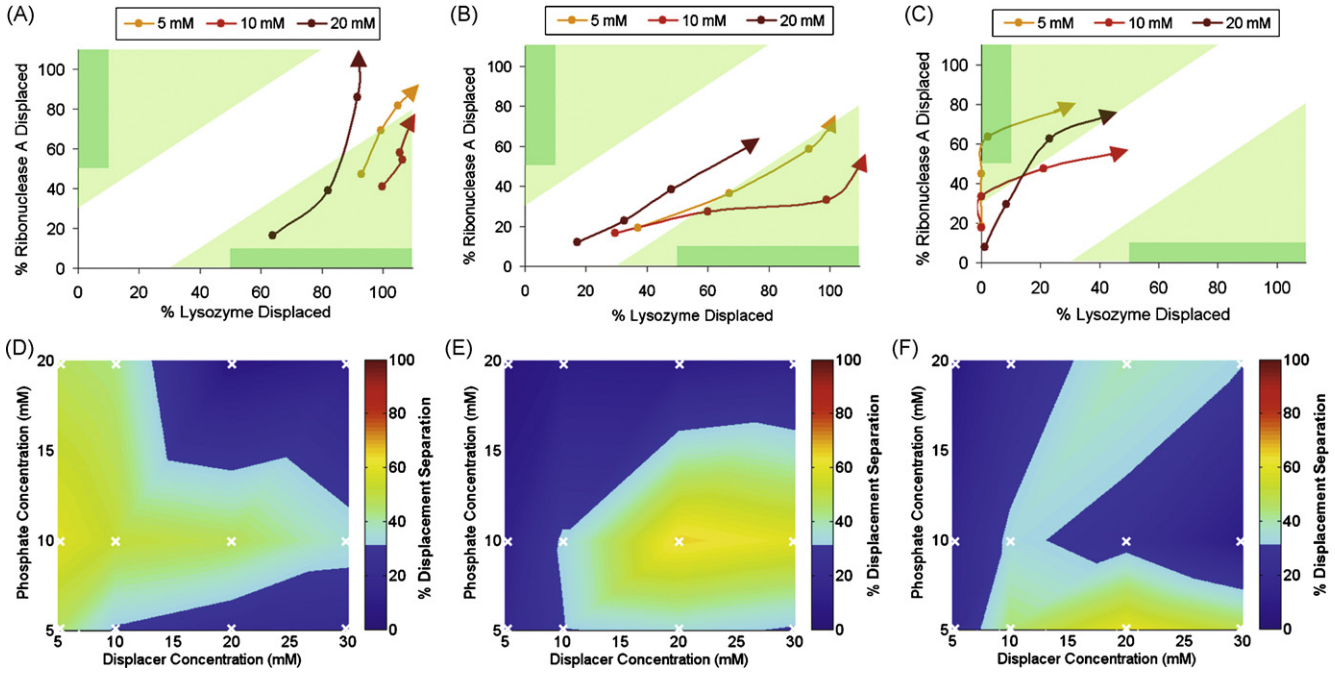

Fig. 7. Batch separation results for RNaseA and Lys using selective displacers at different phosphate concentrations. For the selectivity pathway plots colored arrows denote the different phosphate concentrations used for the experiment, the light green triangular zones denote a selective separation and the dark green rectangular zones denote an exclusive separation. A, B and C correspond to selectivity pathway plots for displacers 8, 16, and 28, respectively. D, E and F correspond to 3D selectivity plots for displacers 8, 16, and 28, respectively. Experimental data points for the 3D selectivity plots are shown by white × marks. (For interpretation of the references to colour in this figure legend, the reader is referred to the web version of the article.)

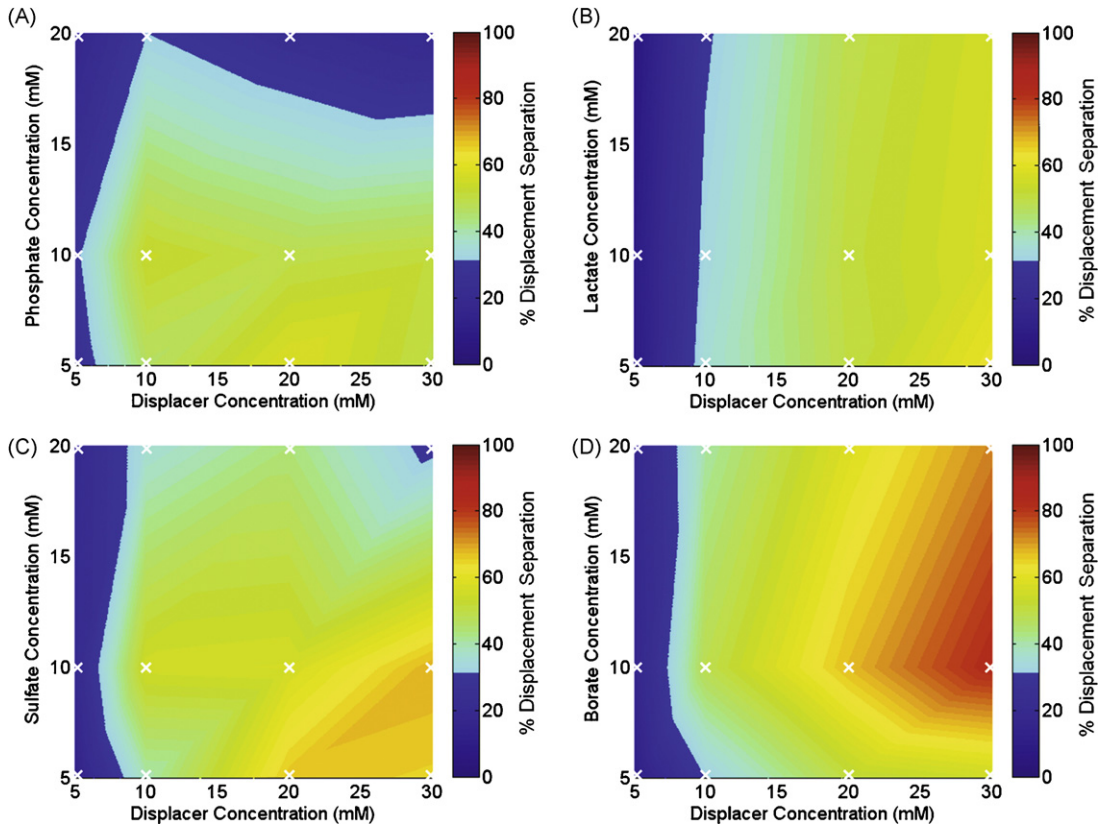

Fig. 8. 3D selectivity plots for the separation of RNaseA and Lys using displacer 28 in different concentrations (5, 10 and 20 mM) of mobile phase modifiers. (A) Monobasic sodium phosphate; (B) lactate; (C) sodium sulfate; (D) borate. For all of these experiments with displacer 28, Lys was retained and RNaseA was displaced. Experimental data points are shown by white × marks.

resenting increasing degrees of selectivity (rainbow scheme from light blue to dark red).

As can be seen in Fig. 7, selective separations were possible in the batch mode using a number of different displacers with Lys and RNaseA. The selective displacers employed in this figure (8, 16 and 28) were all single-interaction moiety displacers. In contrast, several multi-interaction analogues of the selective displacers (e.g. displacers 37, 38 and others not shown) resulted in non-selective separations. This would suggest that selective separations are best carried out using single-interaction type displacers in CHA. Results in Fig. 7 also show a clear dependence on both displacer and phosphate concentration for the selectivity of the separation. For example, in Fig. 7E the optimum conditions for a selective separation occurred at 20 mM displacer and 10 mM phosphate. Further, it can be seen in Fig. 7D–F that these separation were quite sensitive to the conditions, with a rapid decrease in selectivity occurring with small changes in operating conditions.

The selectivity of these separations was also seen to be a strong function of the displacer design. While displacers 8 and 16 (which are amine based) selectively displaced Lys, displacer 28 (which is carboxyl based) selectively displaced RNaseA. This is most likely due to the relative importance of the different binding modes used by Lys and RNaseA on CHA. As shown in Fig. 1, while a sodium chloride gradient resulted in the elution of Lys prior to RNaseA, a phosphate gradient resulted in the elution of RNaseA prior to Lys. Although these proteins were unable to be resolved by either gradient, the minor differences in gradient elution order suggest that RNaseA had a stronger cationic interaction with CHA and Lys had a stronger metal chelation interaction. Thus, it would be expected that Lys would be more effectively displaced using amine based displacers (e.g. 8 and 16) and that RNaseA would be more effectively displaced using a carboxyl based displacer (e.g. 28). It should be noted that the ability to choose the selectivity order of the proteins based upon the design of the displacer is not possible using a mono-interaction type resin. This represents an important additional element of control available in the selective displacement of proteins from a multi-modal resin such as CHA.

Selective separations in the batch mode were also shown to be possible with several other protein pairs (Table 1) that were inseparable using specific linear gradient conditions in CHA. These results demonstrate that the technique of selective displacement/elution in CHA may be applicable to a wide range of protein separation problems.

3.3.1. *Effect of different mobile phase modifiers on selectivity*

As was shown in Fig. 7, phosphate concentrations were found to significantly affect the overall selectivity of the separations. This was due to phosphate's ability to directly mitigate metal chelation interactions with the CHA surface. In order to further investigate this behavior, an additional robotic high-throughput batch screen was carried out using several different mobile phase modifiers (e.g. phosphate, lactate, sulfate and borate) with each modifier affecting electrostatic and metal chelation interactions differently (see Section 2 for detailed HTS protocol). This screen was carried out on the protein pair Lys/RNaseA using a number of displacers which previously showed selectivity or were analogues of those displacers (e.g. displacers 7, 8, 5, 16, 23, 24, 28 and 38). Representative results shown as 3D selectivity plots for displacer 28 and the four mobile phase modifiers are given in Fig. 8.

As can be seen in Fig. 8A, a maximum separation of approximately 60% was achieved using displacer 28 and monobasic sodium phosphate as the mobile phase modifier. For this separation, selectivity was a function of both displacer and phosphate concentrations. Fig. 8B, using lactate as the mobile phase modi-

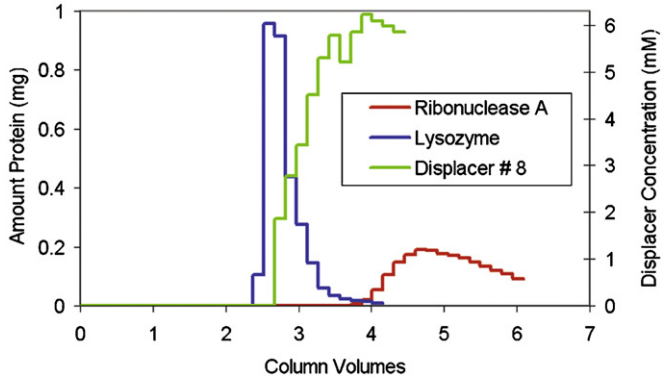

Fig. 9. Selective displacement/elution of Lys and RNaseA using 5 mM displacer 8 (spermidine): column, 121.5 mm × 4.6 mm i.d., CHA resin, type I, 40 μm; carrier, 10 mM sodium phosphate buffer with 50 mM sodium chloride, pH 6.5; protein loading, 3.2 mg each of Lys and RNaseA; flow rate, 0.2 mL/min.

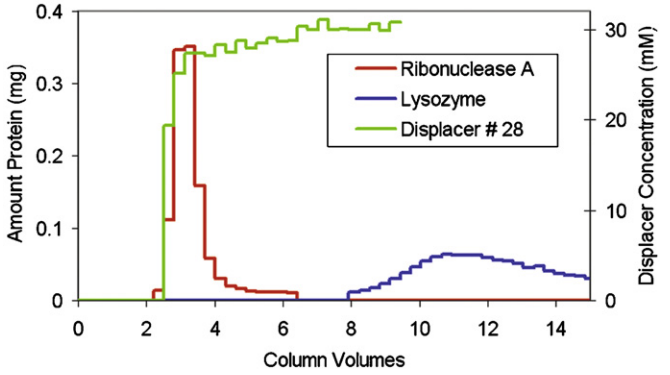

Fig. 10. Selective elution of Lys and RNaseA using 30 mM of displacer 28 (1,2,3,4-butanetetracarboxylic acid): column, 60 mm × 4.6 mm i.d., CHA resin, type I, 40 μm; carrier, 10 mM borate with 5 mM bis–tris and 20 mM sodium chloride, pH 6.5; protein loading, 1 mg each of Lys and RNaseA; flow rate, 0.2 mL/min.

fier, also gave a maximum separation of roughly 60% between Lys and RNaseA. Interestingly, the displacement separation appeared to be relatively insensitive to the lactate concentrations used in the experiment, in contrast to results with the other modifiers. While both phosphate and lactate produced a maximum separation of 60%, the use of sodium sulfate improved the separation to 70% (Fig. 8C). The separation was further improved to nearly 90% when borate was used as the mobile phase modifier (Fig. 8D). These results are quite significant since they demonstrate that a protein pair which was inseparable by linear gradient methods can be almost completely separated in a batch separation through the appropriate combination of a selective displacer/eluent and mobile phase modifier. Clearly the use of different mobile phase modifiers can greatly enhance a given displacement separation. It should also be noted that the order of selectivity (which protein is displaced first) was not changed by using the different mobile phase modifiers. A separate control experiment was carried out to examine if the proteins Lys and RNaseA were able to be resolved using linear gradient methods with these mobile phase modifiers. The results (not shown) indicated that minimal separation of the proteins could be achieved with the mobile phase modifiers alone. Thus, by using a modifier which synergistically complements the selectivity of a given displacer, the overall selectivity of a separation can be greatly increased beyond that achieved using either component alone (displacement or mobile phase modifiers). These results clearly demonstrate the ability of selective displacement/elution to combine the selectivities of multi-modal resins, selective displacers/eluents and mobile phase modifiers to create unique selectivity windows unattainable using traditional modes of operation.

3.4. Selective column displacements/elutions on CHA

Based upon these encouraging results obtained in the batch mode, several selective displacers with appropriate mobile phase modifiers were evaluated in the column mode. The protein pair Lys/RNaseA was again used as a model protein system. Column separations were optimized by varying mobile phase modifier concentrations and with the addition of sodium chloride to the running buffer (*Note*: sodium chloride was added to enable faster desorption kinetics for the proteins and displacer with the CHA surface under column conditions). The resulting column separations of Lys/RNaseA on CHA are shown in Figs. 9 and 10 using displacer 8 with sodium phosphate and displacer 28 with borate, respectively (*Note*: these separations are based upon the batch results shown in Figs. 7A and D and 8D).

As can be seen in Fig. 9, the use of displacer 8 with sodium phosphate resulted in the partial displacement of Lys and the elution of RNaseA. This operation resulted in baseline separation between these proteins which were unable to be separated using linear gradient methods or mobile phase modifiers alone. Further, the selectivity observed in the batch experiments was also attained in the column experiment, with Lys being selectively displaced first.

The use of displacer 28 with borate as the mobile phase modifier resulted in the elution of RNaseA, followed by Lys (Fig. 10). Importantly, baseline separation between the two proteins was achieved by using this combination of selective displacer/eluent and mobile phase modifier in a synergistic fashion. This column result also maintained the selectivity reversal seen previously from the batch results, with RNaseA selectively eluting first from the column. While the order of displacement/elution in these column experiments was determined by the displacer chemistry, the use of appropriate mobile phase modifiers further improved these separations.

The results shown in Figs. 9 and 10 indicated that while excellent separation between the proteins was achieved, these separations did not result in full displacements of the proteins. A range of sodium chloride concentrations were examined with these separations, and in all cases, full displacement was not possible using the CHA resin system. In addition, the use of elevated sodium chloride concentrations was also shown to adversely affect the separations. These results suggest that a single-interaction mode displacer (such as displacers 8, 16 and 28) may be unable to achieve full protein displacement since they have only one interaction mode on CHA. In order to achieve full displacement, a protein must be effectively displaced from the resin due to competitive adsorption. For multimodal systems such as CHA, this would require all interactions of the protein with the resin to be affected by the displacer, thus necessitating a multi-interaction displacer. However, due to charge repulsion effects in CHA, multi-interaction displacers were found to be both ineffective as displacers and non-selective in the batch mode. Thus, for CHA resins, full displacement may not be possible. On the other hand, full selective displacement may be possible on other multi-modal resin systems which have interaction modes that are mutually exclusive (e.g. Capto MMA and MMC).

While full displacement was not achieved in CHA, the selective displacement/elutions resulted in excellent separation of the proteins. In fact, it is quite striking that the same resin material could result in such dramatically different separations through the use of an appropriate displacer/eluent and mobile phase modifier. Thus, not only were we able to achieve baseline separation for proteins that could not be separated using traditional methods, but we were able to also reverse the elution order in these systems while still maintaining baseline separations.

4. Conclusion

A fundamental study on displacer design for CHA and the development of highly selective separations was carried out. A robotic liquid handling system was employed to carry out a parallel batch screen on a displacer library made up of analogous compounds. By incorporating positively charged, metal chelating and/or hydrogen bonding groups into the design of the displacer specific interaction sites on CHA were targeted, thereby augmenting the selectivity of the separation. Important functional group moieties and trends for the design of a CHA displacer were established. An increased separation distance between carboxyl groups was found to afford a higher displacer efficacy, due to better alignment with the fixed calcium sites on the CHA surface. On the other hand, a decreased separation distance between positively charged groups was found to produce a higher displacer efficacy, probably due to increased charge density on the displacer facilitating electrostatic interaction with the resin. Displacers which employed both cation exchange and metal chelation interactions were found to be less efficacious than displacers which used only one mode of interaction, most likely due to charge repulsion effects.

Selective batch separations were achieved between multiple protein pairs using appropriate displacers/eluents which were unable to be resolved using linear gradient techniques in CHA. Interestingly, the specific interaction moieties used on the selective displacer were found to dictate which protein was selectively displaced in the separation, a degree of control not possible using a mono-interaction type resin in displacement chromatography. The effects of different mobile phase modifiers, such as phosphate, sulfate, lactate and borate, were also investigated in these batch displacement systems and were shown to play a crucial role, effectively augmenting the selectivity of the separation. In fact, a selective batch separation of 90% was achieved between Lys and RNaseA, a protein pair which was unable to be resolved using linear gradient techniques or mobile phase modifiers alone. Column separations were then carried out using identified selective displacers and mobile phase modifiers. While full displacement was not achieved in CHA, the selective displacement/elutions resulted in excellent separation of the proteins in the column mode. In addition, not only were we able to achieve baseline separation for proteins that could not be separated using traditional methods, but we were able to also reverse the elution order in these systems while still maintaining baseline separations.

This work demonstrates the potential of selective displacement/elution chromatography to synergistically combine the selectivities of multi-modal resins, displacers/eluents and mobile phase modifiers to create unique selectivity windows unattainable using traditional modes of operation. This proof of concept study now opens up the possibility of applying this new class of separations to different multi-modal resin systems and a variety of important applications. Further, this work raises several interesting questions with respect to the mechanisms and modes of synergy for these combined processes. Future work in our laboratory will involve fundamental studies into how competitive binding of selective displacers/eluents works in concert with mobile phase modifiers in multi-modal resin systems to create these unique selectivity windows for protein separations.

Acknowledgements

This work was partially supported by Bio-Rad, Inc. and NSF Grants CBET-0730830 and CBET 0933169. We would like to acknowledge Mark Snyder of Bio-Rad, Inc. for his assistance in regeneration protocols for ceramic hydroxyapatite columns.

Appendix A. Supplementary data

Supplementary data associated with this article can be found, in the online version, at doi:10.1016/j.chroma.2010.08.038.

References

[1] J. Frenz, C. Horvath, High Performance Chromatography—Advances and Perspectives: High Performance Displacement Chromatography, Academic Press, San Diego, 1998.
[2] S. Vogt, R. Freitag, Journal of Chromatography A 760 (1997) 125.
[3] R. Freitag, J. Breier, Journal of Chromatography A 691 (1995) 101.
[4] A.A. Shukla, K.M. Sunasara, R.G. Rupp, S.M. Cramer, Biotechnology and Bioengineering 68 (2000) 672.
[5] K.A. Barnthouse, W. Trompeter, R. Jones, P. Inampudi, R. Rupp, S.M. Cramer, Journal of Biotechnology 66 (1998) 125.
[6] J.A. Gerstner, J. Morris, T. Hunt, R. Hamilton, N.B.J. Afeyan, Journal of Chromatography A 695 (1995) 195.
[7] A.A. Shukla, R.L. Hopfer, D.N. Chakravarti, E. Bortell, S.M. Cramer, Biotechnology Progress 14 (1998) 92.
[8] A. Kundu, S.M. Cramer, Analytical Biochemistry 248 (1997) 111.
[9] G. Jayaraman, S.D. Gadam, S.M. Cramer, Journal of Chromatography 630 (1993) 53.
[10] E.A. Peterson, A.R. Torres, Analytical Biochemistry 130 (1983) 271.
[11] G. Jayaraman, Y. Li, J.A. Moore, S.M. Cramer, Journal of Chromatography A 702 (1995) 143.
[12] A.A. Shukla, R.R. Deshmukh, J.A. Moore, S.M. Cramer, Biotechnology Progress 16 (2000) 1064.
[13] N. Tugcu, R.R. Deshmukh, Y.S. Sanghvi, J.A. Moore, S.M. Cramer, Journal of Chromatography A 923 (2001) 65.
[14] J. Liu, S.K. Park, J.A. Moore, S.M. Cramer, Industrial & Engineering Chemistry Research 45 (2006) 9107.
[15] A. Kundu, S. Vunnum, S.M. Cramer, Biotechnology and Bioengineering 48 (1995) 452.
[16] A. Kundu, S. Vunnum, S.M. Cramer, Journal of Chromatography A 707 (1995) 57.
[17] K. Rege, S. Hu, J.A. Moore, J.S. Dordick, S.M. Cramer, Journal of the American Chemical Society 126 (2004) 12306.
[18] J. Liu, Z.A. Hilton, S.M. Cramer, Analytical Chemistry 80 (2008) 3357.
[19] C.J. Morrison, S.K. Park, C. Simocko, S.A. McCallum, S.M. Cramer, J.A. Moore, Journal of the American Chemical Society 130 (2008) 17029.
[20] C.J. Morrison, R. Godawat, S.A. McCallum, S. Garde, S.M. Cramer, Biotechnology and Bioengineering 102 (2009) 1428.
[21] C.J. Morrison, C.M. Breneman, J.A. Moore, S.M. Cramer, Analytical Chemistry 81 (2009) 6186.
[22] C.J. Morrison, S.M. Cramer, Biotechnology Progress 25 (2009) 825.
[23] C.A. Brooks, S.M. Cramer, AIChE Journal 38 (1992) 1969.
[24] C.A. Brooks, S.M. Cramer, Chemical Engineering Science 51 (1996) 3847.
[25] S.D. Gadam, G. Jayaraman, S.M. Cramer, Journal of Chromatography 630 (1993) 37.
[26] S.D. Gadam, S.M. Cramer, Chromatographia 39 (1994) 409.
[27] S.D. Gadam, S.R. Gallant, S.M. Cramer, AIChE Journal 41 (1995) 1676.
[28] S.R. Gallant, S. Vunnum, S.M. Cramer, AIChE Journal 42 (1996) 2511.
[29] G. Jayaraman, Y. Li, A. Kundu, J.A. Moore, S.M. Cramer, Biotechnology Advances 15 (1997) 749.
[30] A. Kundu, A.A. Shukla, K.A. Barnthouse, J.A. Moore, S.M. Cramer, Biopharm 10 (1997) 64.
[31] A. Kundu, S. Vunnum, S.M. Cramer, Adsorption-Journal of the International Adsorption Society 4 (1998) 373.
[32] A. Ladiwala, K. Rege, C.M. Breneman, S.M. Cramer, Langmuir 19 (2003) 8443.
[33] C.B. Mazza, C.E. Whitehead, C.M. Breneman, S.M. Cramer, Chromatographia 56 (2002) 147.
[34] J.A. Moore, Cramer, S.M., Tugcu, N., Park, S.K., in, USA, 2005.
[35] K. Rege, A. Ladiwala, N. Tugcu, C.M. Breneman, S.M. Cramer, Journal of Chromatography A 1003 (2004) 19.
[36] A.A. Shukla, S.S. Bae, J.A. Moore, K.A. Barnthouse, S.M. Cramer, Industrial & Engineering Chemistry Research 37 (1998) 4090.
[37] N. Tugcu, S.K. Park, J.A. Moore, S.M. Cramer, Industrial & Engineering Chemistry Research 41 (2002) 6482.
[38] N. Tugcu, R.R. Deshmukh, Y.S. Sanghvi, S.M. Cramer, Reactive and Functional Polymers 54 (2003) 37.
[39] P. Gagnon, P. Ng, J. Zhen, C. Aberin, J. He, H. Mekosh, L. Cummings, S. Zaidi, R. Richieri, BioProcess International (2006) 50.
[40] P. Gagnon, Journal of Immunological Methods 336 (2008) 222.
[41] P.K. Ng, J. He, A. Cohen, Bio-Rad (2006).
[42] M.J. Gorbunoff, Analytical Chemistry 136 (1984) 425.
[43] M.J. Gorbunoff, Analytical Chemistry 136 (1984) 433.
[44] M.J. Gorbunoff, S.N. Timasheff, Analytical Chemistry 136 (1984) 440.
[45] P.K. Ng, J. He, P. Gagnon, Journal of Chromatography A 1142 (2007) 13.
[46] C. Kasper, J. Breier, S. Vogt, R. Freitag, Bioseparations 6 (1996) 247.

[47] R. Freitag, S. Vogt, M. Modler, Biotechnology Progress 15 (1999) 573.
[48] T. Kawasaki, Journal of Chromatography 544 (1991) 147.
[49] M.I. Kay, R.A. Young, A.S. Posner, Nature 204 (1964) 1050.
[50] G. Ma, X.Y. Liu, Crystal Growth & Design 9 (2009) 2291.
[51] Cambridgesoft, in, CS Chem3D Ultra 7.0, Cambridge, MA.
[52] P. Gagnon, C.W. Cheung, P.J. Yazaki, Journal of Separation Science 32 (2009) 1.
[53] ChemAxon TM, in, http://www.chemaxon.com/marvin/sketch/index.html, 2008.